Polymer 51 (2010) 2286–2295

Contents lists available at ScienceDirect

Polymer

journal homepage: www.elsevier.com/locate/polymer

Synthesis and characterization of bioactive molecules grafted on poly(ε-caprolactone) by "click" chemistry

Jiraphong Suksiriworapong [a], Kittisak Sripha [b,*], Varaporn Buraphacheep Junyaprasert [a]

[a] Department of Pharmacy, Faculty of Pharmacy, Mahidol University, Bangkok 10400, Thailand
[b] Department of Pharmaceutical Chemistry, Faculty of Pharmacy, Mahidol University, Bangkok 10400, Thailand

ARTICLE INFO

Article history:
Received 1 December 2009
Received in revised form
18 March 2010
Accepted 21 March 2010
Available online 27 March 2010

Keywords:
Bioactive molecules
Poly(ε-caprolactone)
Click chemistry

ABSTRACT

A facile and efficient strategy to graft bioactive molecules (nicotinic acid, *p*-aminobenzoic acid, and phthaloyltryptophan) onto poly(ε-caprolactone) (P(εCL)) was achieved by copper-catalyzed Huisgen's 1,3-dipolar cycloaddition known as click reaction. P(αClεCL), with 10, 20, and 30% of α-chloro-ε-caprolactone (αClεCL) units were copolymerized by ring opening polymerization using εCL and αClεCL as starting materials in the presence of 1,4-butanediol and $Sn(Oct)_2$. Subsequently, the chloride pendent was converted to azide followed by cycloaddition with terminal alkyne derivatives of the aforementioned bioactive molecules. The complete addition was accomplished at all ratios. The characteristic molecular features of these copolymers were evaluated by FTIR, NMR, and GPC. Thermal analysis data indicated that the grafted compounds led to polymorphic alteration and different pattern of thermal degradation depending on the molecular structure and the size of the grafted compounds. They are the basis for further development of grafted copolymer as drug delivery carriers.

1. Introduction

Over the past decades, research on grafting bioactive molecules onto biodegradable polymer backbones has gained much interest to augment the efficacy of medical and pharmaceutical applications including drug delivery systems, tissue engineering, and medical devices. Various methods have been used to modify biomaterials for drug delivery. In general, drugs or attractive functional groups may be conjugated to polymers [1–6]. But the amount of the conjugated drug is limited since only one drug molecule or group can adhere at one-side of the polymer chain. The other approach is accomplished by substitution of functional groups such as hydroxyl, amino, and carboxylic acid along the polymer backbone. Although this method seems promising, the protic functional groups lead to intra- and intermolecular transesterification resulting in chain degradation and uncontrolled molecular weight [7].

The polyesters poly(lactide), poly(glycolide), and poly(ε-caprolactone) are considered polymers with attractive properties, i.e., biodegradable, biocompatible and environmental friendly properties. Poly(ε-caprolactone) (P(εCL)) has been synthesized and functionalized to enhance its attractive properties. Several methods have been proposed to graft functional groups along the P(εCL) backbone; however, they often encountered limitations such as incomplete conversion [8] or multiple step synthesis [9,10]. Recently, it was reported on the possibility of grafting of functional groups along the P(εCL) through Huisgen's 1,3-dipolar cycloaddition, known as "click chemistry" [11]. This reaction has gained much attention due to its feasible, easy, and mild conditions. Riva et al. [12–14] and Lee et al. [15] demonstrated that small functional groups (i.e., benzoate, triethyl ammonium bromide, hexyne, and proline) and macromolecules (such as Poly(ethylene oxide) (PEO)) could be successfully grafted onto the polymer backbone by the click reaction. In addition, the ligands could be easily conjugated along the polymer backbone with various amounts of grafting units. Although a number of attempts have been made to attach either functional groups or drug molecules on polymer backbones, only a few studies are found concerned with the attachment of drugs onto polyester backbones, in particular onto P(εCL) [16,17].

Therefore the pharmacologically bioactive compounds nicotinic acid, *p*-aminobenzoic acid (PABA) and phthaloyltryptophan [18–25], shown in Fig. 1, were chosen as model compounds for grafting on P(εCL) to evaluate possible interactions between drug molecule and the polymer during the grafting reaction and to compare the physicochemical properties of the resulting copolymers. Contrasting PABA with nicotinic acid, the pendent amino group of PABA in para position is a protic functional group with basic character acting as hydrogen bond donor; however, it exhibits an acidic property according to its pKa (4.65 and 4.8) [26,27]. The

* Corresponding author. Tel./fax: +66 2 644 8677.
E-mail address: pyksp@mahidol.ac.th (K. Sripha).

0032-3861/$ – see front matter Crown Copyright © 2010 Published by Elsevier Ltd. All rights reserved.
doi:10.1016/j.polymer.2010.03.034

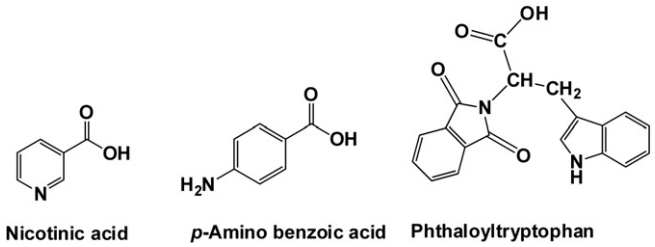

Fig. 1. Structure of bioactive model compounds used in the current study.

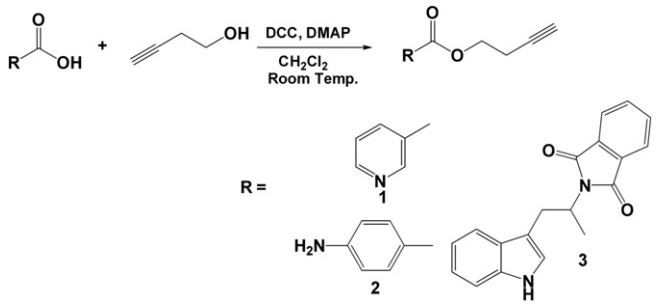

Fig. 2. Esterification of bioactive molecules with 3-butyn-1-ol using coupling reaction (1 = but-3-ynyl nicotinate, 2 = but-3-ynyl 4-aminobenzoate, and 3 = 3(2-N-phthalimido-2-(prop-2-ynyl acetayl)ethyl)indole).

nitrogen atom of the nicotinic pyridine ring on the contrary is solely a hydrogen bond acceptor providing a pair of unshared electrons with basic character. These differences in molecular properties may influence the grafting reaction and affect drug loading and the release characteristic. In addition, the homo- and heteroaromatic rings of these two molecules can display aromatic π−stacking interaction with other loaded drugs in nanoparticles made of these copolymers. The third model drug, phthaloyltryptophan, was selected as an example of a large bioactive compound the bulky structure of which may have steric effects in contrast to the former two drugs.

To the best of our knowledge, there is so far no report on the engrafting of these three bioactive molecules (nicotinic acid, PABA, and phthaloyltryptophan) on P(εCL) by click reaction. Therefore, the aim of this work was to study the synthesis of novel engrafted P(εCL) with these compounds by Huisgen's 1,3-dipolar cycloaddition, and to evaluate its limitation as well as to compare the differing molecular properties of the grafted copolymers including their thermal properties in ratio to their composition.

2. Experimental section

2.1. Materials

ε-Caprolactone (εCL; Aldrich) was dried over CaH_2 for 48 h followed by distillation prior to use. PABA (Aldrich), nicotinic acid (Ajax Finechem), and L-tryptophan (Fluka) were used without any purification. 1,4-Butanediol, 3-butyn-1-ol, α-chlorocyclohexanone, *N*-carbethoxyphthalimide, copper (I) iodide (CuI), 1,8-diazabicyclo [5.4.0]undec-7-ene (DBU), and stannous (II) octanoate ($Sn(Oct)_2$) were obtained from Aldrich Chemicals. *N,N*-dicyclohexylcarbodiimide (DCC), 4-dimethylaminopyridine (DMAP), and *m*-chloroperoxybenzoic acid (*m*CPBA, 70%) were purchased from Fluka. Sodium azide was purchased from Asia Pacific Specialty Chemicals Limited. Dichloromethane (CH_2Cl_2), dimethylformamide (DMF), and tetrahydrofuran (THF) were dried over molecular sieve 4 Å overnight. All other organic solvents were used as received.

2.2. Phthaloylation of tryptophan

The amino group of tryptophan was reacted with *N*-carbethoxyphthalimide according to [28,29]. Briefly, to anhydrous sodium carbonate (0.52 g, 4.90 mmol) dissolved in 10 mL of water was added tryptophan (0.50 g, 2.45 mmol) under stirring. After complete dissolution, *N*-carbethoxyphthalimide (0.59 g, 2.69 mmol) was introduced into the reaction flask. The reaction mixture was further stirred for 2 h at room temperature and then extracted twice with ethyl acetate. The aqueous layer was acidified to pH 2−3 with 1 N hydrochloric acid solution and extracted three times with ethyl acetate. The combined organic layers were dried over anhydrous magnesium sulfate. The solvent was evaporated under reduced pressure after filtration. The residue is then purified by column chromatography on silica gel using a mixture of ethyl acetate (EtOAc), hexane (Hex), and glacial acetic acid (CH_3COOH) (4:1:0.01) as mobile phase. The collected fraction was twice extracted with purified water to eliminate residual acetic acid. The organic layer was then dried again over anhydrous magnesium sulfate, filtered, and evaporated under reduced pressure to yield a yellow solid (0.8 g, 98%); m.p. 172.3 °C; TLC $R_f = 0.13$ (silica gel, EtOAc:Hex:CH_3COOH/4:1:0.01); FTIR (KBr) ν (cm^{-1}) 3408, 3056, 2928, 1774, 1710, 1391, 1104, 1071, 718; ^1H NMR ($CDCl_3$): $\delta = 3.80$ (m, 2H, CH_2CH), 5.35 (m, 1H, CH_2CH), 7.02 (s, 1H, indole), 7.17 (m, 1H, indole), 7.27 (d, 1H, indole), 7.62 (s, 1H, indole), 7.65 (m, 2H, phthaloyl), 7.75 (m, 2H, phthaloyl), 8.03 (s, 1H, NH); MS (EI, 70 eV) *m/z* (rel int) 335 $[M + H]^+$ and 357 $[M + Na]^+$; Anal. Calcd. for $C_{19}H_{14}N_2O_4$: C, 68.26; H, 4.22; N, 8.38; O, 19.14. Found: C, 68.03; H, 4.18; N, 8.29; O, 19.50.

2.3. General procedure for esterification with 3-butyn-1-ol (Fig. 2)

The required amounts of DCC and DMAP were dissolved in (CH_2Cl_2) in a reaction flask. An acidic model compound was added and stirred at room temperature for 30 min 3-Butyn-1-ol was charged through a dried stainless steel syringe under argon atmosphere. The reaction was conducted at room temperature for 24 h. After filtration of the precipitate, the solvent was evaporated under reduced pressure. The crude product was then purified by column chromatography on silica gel.

2.3.1. Synthesis of but-3-ynyl nicotinate (1)

Nicotinic acid (5.0 g, 40.6 mmol), 3.4 g (48.8 mmol) of 3-butyn-1-ol, 12.6 g (61.0 mmol) of DCC, and 7.4 g (61.0 mmol) of DMAP gave according to 2.3 an off-white solid. Purified compound 1 (5.9 g, 83%) was obtained through column chromatography on silica gel with the mobile phase of Hex, EtOAc, and CH_2Cl_2 (1:2:2); m.p. 46.43 °C TLC with $R_f = 0.50$, FTIR (KBr) ν (cm^{-1}): 3264, 2926, 2850, 2119, 1718;

^1H NMR (DMSO-d_6): δ = 2.65 (m, 2H, $CH_2C{\equiv}CH$), 2.86 (t, $J = 2.61$ Hz, 1H, $C{\equiv}CH$), 4.35 (t, $J = 6.48$ Hz, 2H, $COCH_2$), 7.57 (m, 1H, pyridine), 8.28 (td, $J = 7.96$ Hz, 1H, pyridine), 8.80 (s, 1H, pyridine), 9.08 (s, 1H, pyridine);

Table 1
Fed compositions of copolymerization of αClεCL and εCL.

Copolymers	Fed Weight (g)		Fed Mole (mmol)	
	αClεCL	εCL	αClεCL	εCL
P(εCL)	–	2.28	–	20
P(**10**αClεCL-**90**εCL)	0.29	2.05	2	18
P(**20**αClεCL-**80**εCL)	0.59	1.82	4	16
P(**30**αClεCL-**70**εCL)	0.89	1.60	6	14

^{13}C NMR (DMSO-d_6): δ = 18.3 (CH$_2$C≡CH), 62.8 (OCH$_2$C), 72.5 (C≡CH), 80.6 (C≡CH), 123.9 (CHCHCHCCO in pyridine), 125.5 (pyridine-CO), 136.8 (CHCHCHCCO in pyridine), 149.9 (NCHCCO in pyridine), 153.7 (CHNCHCCO in pyridine), 164.5 (C═O).

2.3.2. Synthesis of but-3-ynyl 4-aminobenzoate (2)

PABA (5 g, 36.5 mmol), 3.1 g (43.8 mmol) of 3-butyn-1-ol, 9.0 g (43.8 mmol) of DCC, and 5.3 g (43.8 mmol) of DMAP gave according to 2.3 an off-white solid. Purified compound 2 (4.5 g, 65%) was obtained through column chromatography on silica gel with the mobile phase of Hex and EtOAc (1:1) still as an off-white solid, m.p. 82.34 °C, TLC with R_f = 0.326, FTIR (KBr) ν (cm^{-1}): 3398, 3336, 3288, 1685, 1599;

^{1}H NMR (CDCl$_3$): δ = 2.04 (t, J = 2.5 Hz, 1H, C≡C*H*), 2.65 (td, J = 6.8, 2.6 Hz, 2H, C*H*$_2$C≡CH), 4.09 (s, 2H, NH$_2$), 4.38 (t, J = 6.8 Hz, 2H, COC*H*$_2$), 6.6 (d, J = 8.5 Hz, 2H, benzene), 7.88 (d, J = 8.5 Hz, 2H, benzene);

^{13}C NMR (CDCl$_3$): δ = 19.1 (CH$_2$C≡CH), 62.0 (OCH$_2$C), 69.8 (C≡CH), 80.3 (C≡CH), 113.7 (2C, benzene), 119.2 (benzene-CO), 131.6 (2C, benzene), 151.0 (benzene-NH$_2$), 166.3 (C═O).

2.3.3. Synthesis of 3(2-N-phthalimido-2-(prop-2-ynyl acetayl) ethyl)indole (3)

Phthaloyltryptophan (4.7 g, 14.0 mmol), 1.2 g (16.9 mmol) of 3-butyn-1-ol, 4.4 g (21.1 mmol) of DCC, and 2.6 g (21.1 mmol) of DMAP gave according to 2.3 compound 3 (3.8 g, 70%) as a yellow solid after column chromatography on silica gel with the mobile phase of EtOAc, Hex and CH_2Cl_2 (1:2:3), m.p. 97.17 °C, TLC with R_f = 0.60, FTIR (KBr) ν (cm^{-1}): 3411, 3270, 2120, 1777, 1738, 1714;

^{1}H NMR (CDCl$_3$): δ = 1.85 (t, J = 2.6 Hz, 1H, C≡C*H*), 2.65 (m, 2H, C*H*$_2$C≡CH), 3.65 (d, J = 8.0 Hz, 2H, CHC*H*$_2$-indole), 4.70 (m, 2H, OC*H*$_2$CH$_2$), 5.30 (m, 1H, Phtaloyl-C*H*CH$_2$-indole), 7.00 (s, 1H, C*H*NH in indole), 7.07 (td, J = 7.04, 1.06 Hz, 1H, indole), 7.14 (td, J = 8.07 1.1 Hz, 1 H, indole), 7.27 (dd, J = 8.09, 0.68 Hz, 1H, indole), 7.62 (s, 1H, indole), 7.64 (m, 2H, phthaloyl), 7.75 (m, 2H, phthaloyl), 8.12 (s, 1H, NH);

^{13}C NMR (CDCl$_3$): δ = 18.8 (CH$_2$C≡CH), 24.7 (CHCH$_2$-indole), 52.6 (phthaloyl-CHCOO), 63.2 (COOCH$_2$CH$_2$), 70.0 (C≡CH), 79.5 (C≡CH), 110.8 (indole), 111.1 (indole), 118.4 (indole), 119.4 (indole), 122.0 (indole), 122.6 (indole), 123.3 (2C, phthaloyl), 127.1 (indole), 131.6 (2C, phthaloyl), 134.0 (2C, phthaloyl), 136.0 (indole), 167.5 (2C, phthaloyl), 168.9 (CHCOO).

2.4. Synthesis of α-chloro-ε-caprolactone (αClεCL)

The αClεCL monomer was synthesized according to the method of Lenoir et al. [30] with modification. Briefly, to 12.5 g of *m*CPBA (50.7 mmol) dissolved in CH_2Cl_2 were added 5 g of α-chlorocyclohexanone (37.7 mmol) into the reaction flask. The reaction was conducted at room temperature for 48 h and then cooled down to −20 °C to precipitate the white by-product which was removed by filtration. The filtrate was washed twice both with saturated sodium dithionite solution and with saturated sodium bicarbonate solution, and finally with water. Subsequently, the filtrate was dried over anhydrous magnesium sulfate, filtered, and concentrated under reduced pressure. Finally, the concentrated organic layer was purified by column chromatography on silica gel with the mobile phase Hex and EtOAc (1:3) yielding *αClεCL* (3.9 g, 70%); TLC R_f = 0.35;

^{1}H NMR (CDCl$_3$): δ = 1.85 (m, 3H) 2.15 (m, 3H), 4.25 (m, 1H, COOC*H*$_2$), 4.65 (m, 1H, COOC*H*$_2$), 4.80 (dd, J_d = 2.03 and 7.77 Hz, 1H, C*H*Cl).

2.5. Synthesis of P(αClεCL-ran-εCL)

All glassware was dried in an oven overnight before use. The amounts of αClεCL, and εCL (see Table 1), 18 mg of 1,4-butanediol (0.2 mmol), and 81 mg of Sn(Oct)$_2$ (0.2 mmol) were weighed into the reaction flask, which was evacuated for 15 min followed by purging with argon gas. Then the flask was immersed in an oil bath at 120 °C. After 6 h of polymerization, the copolymer was recovered by precipitation in cold Hex and finally dried in vacuo for 24 h.

In case of P(εCL) synthesis according 2.5, the homopolymerization of εCL (2.28 g) was initiated with 18 mg of 1,4-butanediol and catalyzed by 81 mg of Sn(Oct)$_2$.

2.6. Synthesis of P(αN$_3$εCL-ran-εCL)

The azide substitution to P(αClεCL-*ran*-εCL) was performed according to Riva et al. [12]. Briefly, to 2 g of P(αClεCL-*ran*-εCL) (1

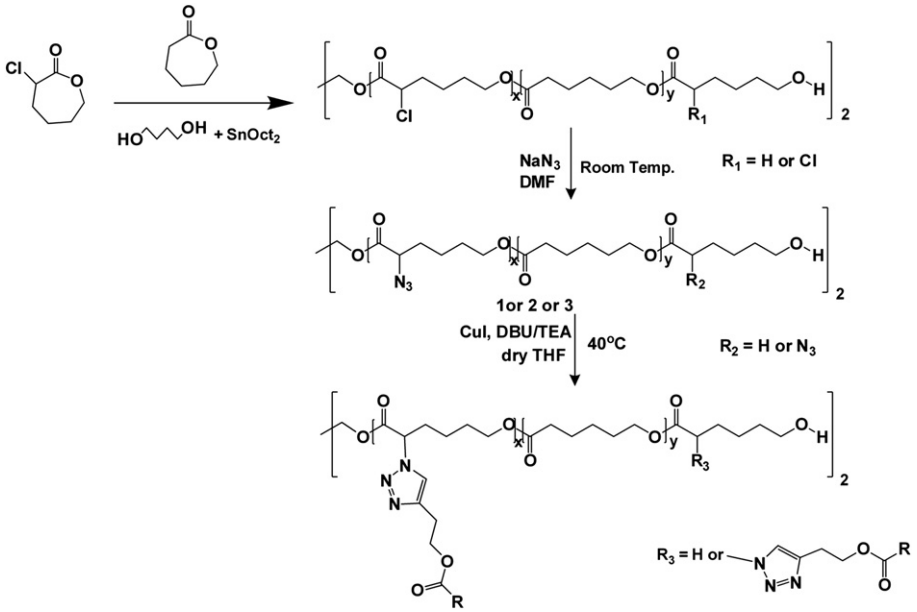

Fig. 3. General scheme for the synthesis of bioactive molecules grafted P(εCL). TEA as base was used for the synthesis of P((PABA-*g*-εCL)-*ran*-εCL.

equiv of αClεCL) dissolved in 5 mL DMF in a flask was added sodium azide (1.02 equiv). The reaction mixture was stirred overnight at room temperature. DMF was then completely evaporated under reduced pressure and the polymeric residue dissolved in toluene. The insoluble salt was centrifuged at 4000 rpm for 15 min. The clear supernatant was evaporated under reduced pressure resulting in the dry copolymer *P(αN$_3$εCL-ran-εCL)*.

2.7. Typical click chemistry reaction

Grafting of bioactive model compounds to P(εCL) backbone was carried out according to literature [12] with some modification. Briefly, 200 mg of P(αN$_3$εCL-*ran*-εCL) (1 equiv of azide) was weighed into a reaction flask containing 5 mL of dry THF. Butynyl-ester derivative of model compound (1, 2, or 3) (1.5 equiv), CuI (0.2 equiv), and base (0.2 equiv) were then loaded into the flask. Under atmospheric argon, the reaction was conducted at 40 °C in a thermostatic bath for 4 h. The grafted copolymer was precipitated in cold Hex and dried in vacuo overnight before characterization.

2.8. Characterizations

^{1}H NMR spectra were recorded in $CDCl_3$ or DMSO-d_6 at 300 or 500 MHz, ^{13}C NMR spectra in $CDCl_3$ or DMSO-d_6 at 75.45 MHz in the FT mode with Bruker Avance 300 apparatus at 25 °C. Infrared spectra were recorded with Jasco FT/IR-4100 spectrophotometer. Number- and weight-average molecular weights (M_n and M_w, respectively) were measured by a Waters 150-CV gel-permeation chromatograph equipped with refractive index detector. THF was used as a mobile phase at a flow rate of 1 mL/min. Two columns of PLgel 10 μm mixed B were calibrated with polystyrene standards in the range of MW between 4490 and 1,112,000 g/mol. Thermal gravimetric analysis (TGA) was carried out with TGA 7 Perkin Elmer thermogravimetric analyzer at 10 °C/min. Differential scanning calorimetry (DSC) was performed using DSC 7 Perkin Elmer differential scanning calorimeter calibrated with indium. Glass transition and melting temperatures (T_g and T_m, respectively) were measured according to running condition: the sample was quenched to −80 °C, heated to 100 °C (first heating), cooled down to −80 °C, and heated again (second heating). Thermograms were recorded during the second heating cycle at 20 °C/min. Mass spectrum was recorded in electron ionization mode at an ion source temperature of 150 °C and an electron energy of 70 eV. Mass spectrum was scanned from 50 to 2000 *m*/*z*.

3. Results and discussion

3.1. Phthaloylation of tryptophan

Tryptophan was phthaloylated prior to conversion to compound 3 through the reaction between tryptophan and *N*-carbethoxyphthalimide under basic condition in high product yield of 98%. ^{1}H and ^{13}C NMR data agreed with those of the literature [31,32]. The melting point was checked by DSC and the onset of T_m was found to be 172.83 °C. CHN elemental analysis and mass spectrum agreed with the theoretical structure. In FTIR spectrum, the phthaloylation of amino group was characterized by disappearance of the strong primary N–H stretching peak of tryptophan at 3400 cm^{-1}; however, the weak secondary N–H stretching peak of indole was still observed. The two bands of C=O stretching at 1710 and 1774 cm^{-1} confirmed the two carbonyls of phthaloyl group. The peak of C=O stretching of the carboxylic acid at 1710 cm^{-1} was overlapped by that of the phthaloyl group.

3.2. Synthesis of esterified model compounds

Typically, highly regioselective copper-mediated 1,3-dipolar cycloaddition between an azide group and a terminal alkyne requires an access of 1,2,3 triazoles [33]. Thus, in this study the feasible pathway was to fix the azido group onto the polymer

Table 2
Molecular characteristic results of copolymers and grafted copolymers.

Copolymers/Grafted copolymers[a]	αClεCL or αN$_3$ or R–C≡CH]/[εCL] Molar Ratio in Feed	[αClεCL or αN$_3$ or R–C≡CH]/[εCL] Calculated Molar Ratio[b] ($F_{grafted}$)	% Yield	$M_{n,theo}$[c]	$M_{n,NMR}$[b]	$M_{n,GPC}$[d]	M_w/M_n[d]
P(εCL)	–	–	95.43	11,400	7737	9396	1.90
P(αClεCL-*ran*-εCL)							
P(**10**αClεCL-**90**εCL)	0.1	0.07	93.83	11,745	8902	10,805	1.96
P(**20**αClεCL-**80**εCL)	0.2	0.17	76.66	12,090	9085	9927	2.24
P(**30**αClεCL-**70**εCL)	0.3	0.25	88.89	12,435	6684	7550	2.20
P(αN$_3$εCL-*ran*-εCL)							
P(**10**αN$_3$εCL-**90**εCL)	0.1	0.09	87.53	11,810	9258	9869	2.09
P(**20**αN$_3$εCL-**80**εCL)	0.2	0.18	78.78	12,220	10,226	9266	2.29
P(**30**αN$_3$εCL-**70**εCL)	0.3	0.28	73.33	12,630	8852	7133	2.27
P((Nico-*g*-εCL)-*ran*-εCL)							
P((**10**Nico-*g*-εCL)-**90**εCL)	0.1	0.07	80.84	13,185	8034	11,246	1.70
P((**20**Nico-*g*-εCL)-**80**εCL)	0.2	0.14	98.25	17,450	8731	7960	1.83
P((**30**Nico-*g*-εCL)-**70**εCL)	0.3	0.24	98.11	17,059	5155	5675	1.62
P((PABA-*g*-εCL)-*ran*-εCL)							
P((**10**PABA-*g*-εCL)-**90**εCL)	0.1	0.06	98.56	13,321	12,533	10,455	1.88
P((**20**PABA-*g*-εCL)-**80**εCL)	0.2	0.15	97.55	17,863	13,098	19,663	1.53
P((**30**PABA-*g*-εCL)-**70**εCL)	0.3	0.25	96.34	17,460	11,052	18,047	1.75
P((Phatryp-*g*-εCL)-*ran*-εCL)							
P((**10**Phatryp-*g*-εCL)-**90**εCL)	0.1	0.07	94.70	15,237	19,789	13,982	1.56
P((**20**Phatryp-*g*-εCL)-**80**εCL)	0.2	0.17	93.12	22,262	21,708	15,858	1.87
P((**30**Phatryp-*g*-εCL)-**70**εCL)	0.3	0.27	95.14	23,099	24,788	12,029	1.88

[a] Abbreviations: Nico = nicotinic acid, PABA = *p*-aminobenzoic acid, Phatryp = phthaloyltryptophan.

[b] Determined by ^{1}H NMR spectroscopy.

[c] $M_{n,theo} = \left(\frac{[\varepsilon CL]}{[I]} \times 114\right) + \left(\frac{[\alpha ClεCL]\text{or}[\alpha N_3 \varepsilon CL]\text{or}[\text{Alkyne}]}{[I]} \times M_{n,\alpha ClεCL \text{ or } \alpha N_3 \varepsilon CL \text{ or Alkyne}}\right)$ This value was calculated based on 100% conversion of monomer; where [*εCL*] is the molar concentration of εCL, [*αClεCL or αN$_3$εCL or alkyne*] is the molar concentration of αClεCL and αN$_3$εCL and alkyne, respectively. [*I*] is the molar concentration of the initiator (1,4-butanediol), and $M_{n,\alpha ClεCL \text{ or } \alpha N_3 \varepsilon CL \text{ or alkyne}}$ is the molecular weight of αClεCL and αN$_3$εCL and alkyne, respectively.

[d] Determined by GPC.

backbone (Fig. 3) and to esterify the model compound acids with 3-butyn-1-ol using the coupling reaction with DCC and DMAP as coupling reagents (Fig. 2) to provide terminal alkynyl ester derivatives, which were characterized by NMR and FTIR spectroscopy as described below.

3.2.1. Synthesis of but-3-ynyl nicotinate (1)

Under aforementioned conditions, but-3-ynyl nicotinate was obtained in 83% yield. Compound 1 was identified by ^{1}H NMR using DMSO-d_6 as solvent. The presence of the methyne proton signal of the terminal alkyne at 2.86 ppm and signal group of the methylene protons adjacent to the oxygen atom of ester group at 4.35 ppm in the spectrum confirmed the structure of but-3-ynyl nicotinate. This result was further verified by a FTIR spectrum. The C–H stretching peak of the terminal alkyne and C=O stretching band of ester carbonyl were identified at 3264 and 1718 cm^{-1}, respectively. Also a weak signal of the C≡C stretching was observed at 2119 cm^{-1}.

3.2.2. Synthesis of but-3-ynyl 4-aminobenzoate (2)

The coupling reaction according to *3.2* between PABA and 3-butyn-1-ol gave but-3-ynyl 4-aminobenzoate in 65% yield. Compound 2 was identified by ^{1}H NMR in $CDCl_3$. The spectrum showed again the typical signal groups for the methylene protons (COOC*H*$_2$) at 4.38 ppm and the methyne proton (C≡C*H*) at 2.04 ppm. The FTIR spectrum recorded in the KBr disc mode showed also the C–H stretching of the terminal alkyne at 3288 cm^{-1} and, in addition, the N–H stretching of the anilino group around 3400 cm^{-1}. The peaks at 1685 and 1599 cm^{-1} were assigned to the C=O stretching and N–H bending, respectively.

3.2.3. Synthesis of 3(2-N-phthalimido-2-(prop-2-ynyl acetayl) ethyl)indole (3)

Phthaloyltryptophan (see *3.1*) was esterified with 3-butyn-1-ol to provide the terminal alkyne functional group according to *3.2* in 70% yield. Compound 3 was identified by ^{1}H NMR in $CDCl_3$. The spectrum exhibited the characteristic signal group for the methylene protons (COOC*H*$_2$) at 4.70 ppm of the ester linkage and that of the alkyne proton at 1.85 ppm. The FTIR spectrum showed the corresponding C–H stretching of the C≡*CH* group at 3270 cm^{-1} and the C=O stretching peak at 1738 cm^{-1}.

3.3. Synthesis of P(αClεCL-ran-εCL)

The αClεCL unit was copolymerized at various molar ratios (0.10, 0.20, and 0.30) with εCL monomer by ring opening polymerization in the presence of the initiator 1,4-butanediol and the catalyst Sn(Oct)$_2$ (Fig. 3). The molar ratio of monomer to initiator and to catalyst, respectively, was set to 100 each. The yield of the copolymers was in each case higher than 70% with molar ratios of the αClεCL units calculated from ^{1}H NMR which were in agreement with the theoretical values.

The $M_{n,theo}$ values were calculated based on 100% conversion of the monomer, the $M_{n,NMR}$ values in Table 2 according to [30] with some modification. Both sets differ to a large extent from each other. This fact might be explained by the electron withdrawing property of the chloride atom in αClεCL leading to a higher reactivity of its lactone moiety in comparison to that of εCL. This caused additional inter- and intramolecular transesterifications during the optimized polymerization process at the high temperature of 120 °C, which were particularly inevitable at the high 0.3 ratio of αClεCL versus εCL. The complete molecular parameter set of the copolymers and grafted copolymers are compiled in Table 2.

3.4. Synthesis of P(αN$_3$εCL-ran-εCL)

Conversion of the chloride pendants to azides was done prior to grafting the model compounds along the polymer chain. P(αClεCL-*ran*-εCL) was substituted with sodium azide in DMF at room temperature (Fig. 3) in an overnight reaction. The ^{1}H NMR spectrum confirmed the complete conversion by means of the azide methine signal (C*H*N$_3$) at 3.85 ppm and the entire disappearance of methyne proton signal (C*H*Cl) at 4.25 ppm. The azide group was also monitored by FTIR by means of the characteristic band at 2100 cm^{-1}. The molecular weight of P(αN$_3$εCL-*ran*-εCL) was slightly increased due to the azide substitution compared to that of P(αClεCL-*ran*-εCL) (Table 2).

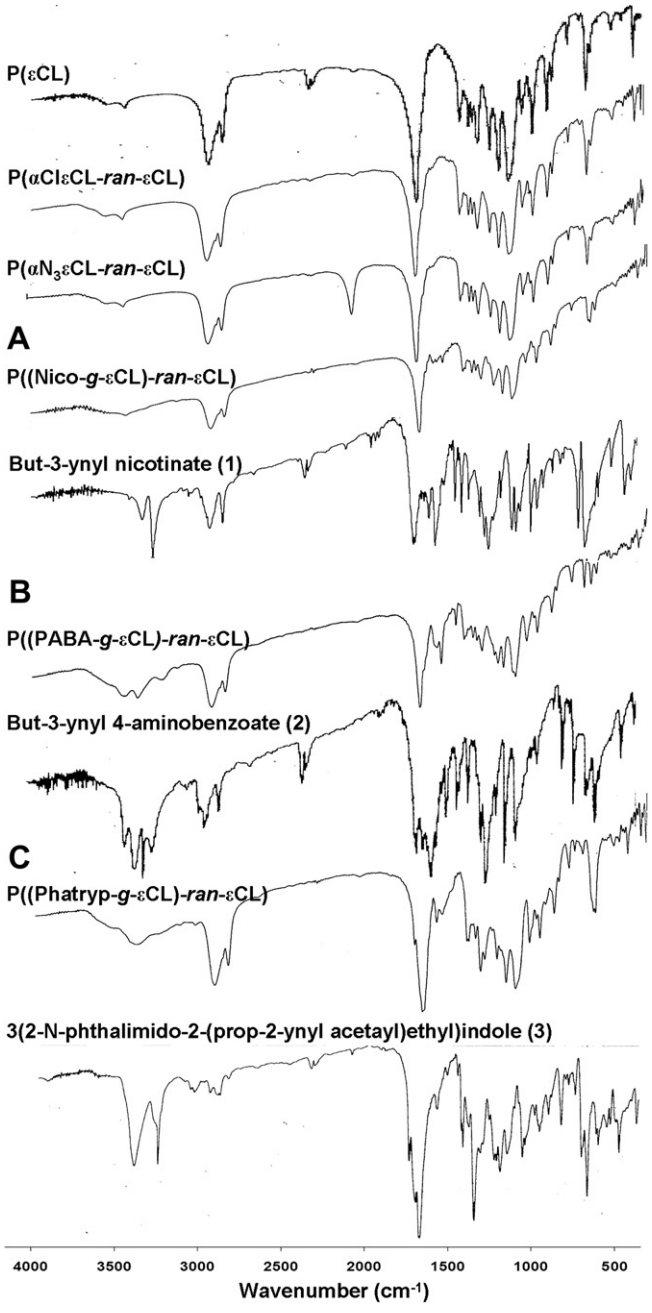

Fig. 4. FTIR spectra of P((Nico-*g*-εCL)-*ran*-εCL) (A), P((PABA-*g*-εCL)-*ran*-εCL) (B), and P((Phatryp-*g*-εCL)-*ran*-εCL) (C), respectively, in comparison with P(εCL) homopolymer, P(αClεCL-*ran*-εCL), P(αN$_3$εCL-*ran*-εCL), and alkyne terminated drug molecules. DBU as base was used for the syntheses of (A) and (C), respectively, whereas TEA for that of (B).

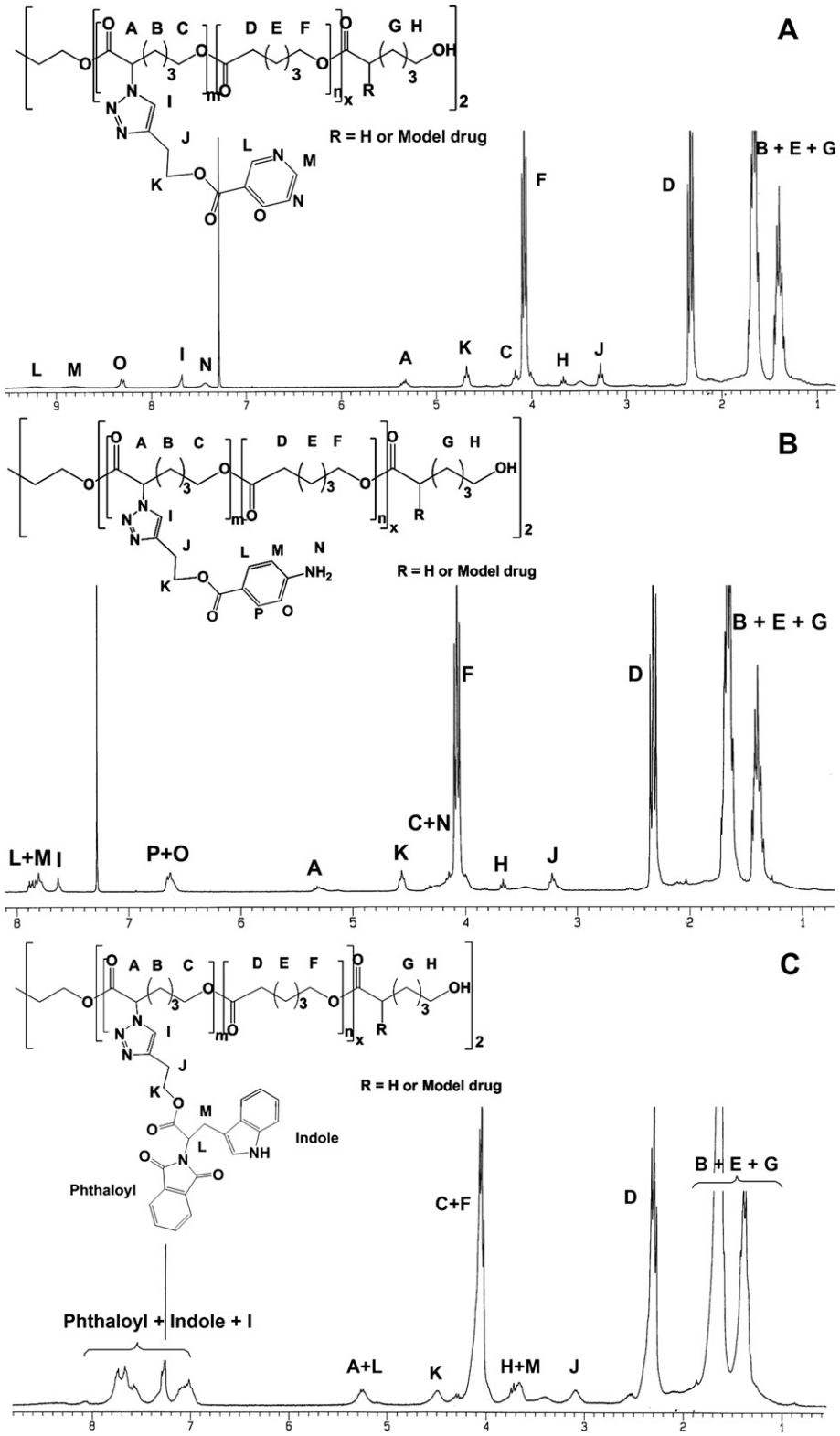

Fig. 5. ^{1}H NMR spectra of P((Nico-*g*-εCL)-*ran*-εCL) (A), P((PABA-*g*-εCL)- *ran*-εCL) (B), and P((Phatryp-*g*-εCL)-*ran*-εCL) (C), respectively. DBU as base was used for the syntheses of (A) and (C), respectively, whereas TEA for that of (B).

3.5. Engrafting of model compounds along P(αN$_3$εCL-ran-εCL) by click reaction

The 3-butynyl ester derivatives of the three model compounds nicotinic acid, PABA, and phthaloyltryptophan were engrafted onto P(αN$_3$εCL-*ran*-εCL) backbone through copper-catalyzed Huisgen's 1,3-dipolar cycloaddition reaction at 40 °C using CuI as catalyst and DBU as base, (Fig. 3). Under monitoring by FTIR, the reaction was completed after 4 h with the complete disappearance of azide peak at 2100 cm^{-1} indicating the entire conversion of the pendent azide

to the triazole ring which showed the characteristic peak at 1610 cm^{-1}. Fig. 4 illustrates the FTIR spectra of all grafted copolymers. In addition, the ^1H NMR spectrum confirmed the cycloaddition by the methyne proton signal of the triazole ring at 7.7 ppm and the disappearance of the methyne proton signal of azide (CHN_3) at 3.85 ppm.

The average molecular weight ($M_{n,NMR}$) of the grafted copolymers and the molar fraction ($F_{grafted}$) of the engrafted model compounds were calculated according to equation (1) and 2, where I represents the integration of the respective ^1H NMR peaks assigned in Fig. 5, and M the molecular weight of compound 1, 2, 3 (M_{alkyne}), and the caprolactone unit ($M_{\varepsilon CL}$), respectively. All values are summarized in Table 2 together with the calculated grafting efficiencies ($F_{grafted}$) which were higher than 80%.

Equation (1)

For nicotinic acid and PABA grafted P(εCL)

$$M_{n,NMR} = \frac{\left[I_A \times M_{alkyne}\right] + \left[\frac{1}{2}I_D \times M_{\varepsilon CL}\right]}{\frac{1}{4}I_H}$$

For phthaloyltryptophan grafted P(εCL)

$$M_{n,NMR} = 2 \times \left(\frac{\left[I_{A+L} \times M_{alkyne}\right] + \left[I_D \times M_{\varepsilon CL}\right]}{I_{H+M} - I_{A+L}} \right)$$

Equation (2)

For nicotinic acid and PABA grafted P(εCL)

$$F_{grafted-CL} = \frac{I_A}{\frac{1}{2}I_D + I_A}$$

For phthaloyltryptophan grafted P(εCL)

$$F_{grafted-CL} = \frac{I_{A+L}}{I_D + I_{A+L}}$$

3.5.1. Grafting of but-3-ynyl nicotinate (1) along the P(εCL) backbone

But-3-ynyl nicotinate (1) was successfully grafted onto the polymer backbone. Fig. 5A shows the ^1H NMR spectrum of nicotinic acid grafted P(εCL) with the characteristic peak of methyne proton of caproyl unit adjacent to the triazole ring at 5.30 ppm (peak A), while the former signal of the methyne proton adjacent to the azide at 3.85 ppm was missing. Further new peaks at 7.45, 8.30, 8.70 and 9.25 ppm were assigned to the protons of nicotinic pyridine ring. These results were confirmed by characteristic peaks of C=C stretching at 1590 cm^{-1}, and of C=N stretching at 1625 cm^{-1} in the FTIR spectrum originating from the overlapping vibrations of the C=N bonds of the triazole and pyridine rings (Fig. 4A).

The molecular weights of the grafted polymers declined only to a minor extent as compared to those of P(αN$_3$εCL-*ran*-εCL) and P(αClεCL-*ran*-εCL) (Table 2). In case of the grafted nicotinic acid, at low percent grafting, the M_n value was remarkably lower for 30% grafting. However, the molecular weight distribution was narrower than those of the original polymers and the value of M_w/M_n and GPC chromatogram showed a unimodal peak (data not shown). If one considers the difference of $M_{n,theo}$ and $M_{n,NMR}$, degradation must have occurred. The nitrogen atom of the nicotinic pyridine ring acts as an intramolecular nucleophile with its localized lone pair electron, cleaving the ester bond by attacking the carbonyl group during the grafting step independent of the strength of the base used. Therefore the extent of polymer degradation could not be minimized, yielding short polymer units which could not be precipitated by cold hexane. This, finally, explains the unimodal GPC peak.

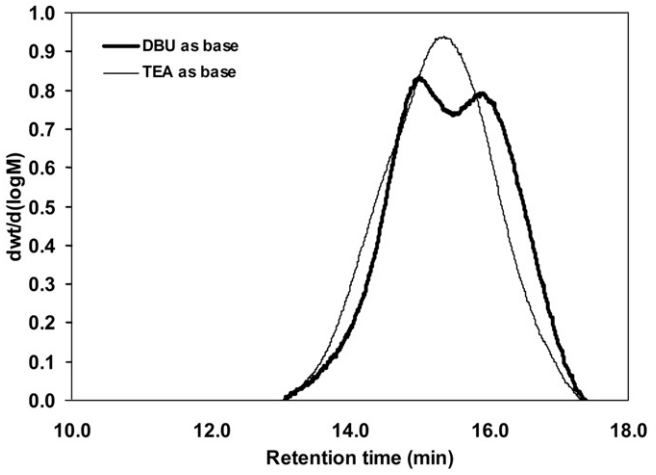

Fig. 6. GPC chromatograms of P((PABA-*g*-εCL)-*co*-εCL) at 30% mole of PABA representing the products of the cycloaddition with TEA and DBU (—,▪),respectively, as base.

3.5.2. Grafting of but-3-ynyl 4-aminobenzoate (2) along the P(εCL) backbone

For grafting *but-3-ynyl 4-aminobenzoate (2)* onto the polymer backbone, DBU was initially used and acted as a base in the cycloaddition reaction. Similar to grafting of nicotinic acid, the reaction was complete after 4 h. At 10% grafting, the corresponding grafted copolymer was attainable without degradation as seen by an increase in $M_{n,GPC}$ without broadening the polydispersity index of molecular weight (PDI) compared to that of P(10αN$_3$εCL-*ran*-εCL). Once the percent grafting of *but-3-ynyl 4-aminobenzoate (2)* was increased to 20 and 30% in the presence of the strong non-nucleophilic, sterically hindered base DBU [34,35], the PDI grew dependently, only slightly raised for the 20% grafting copolymer (data not shown). In contrast, for 30% grafting the GPC chromatogram showed a bimodal peak (Fig. 6), indicating a heterodispersed molecular weight arising from polymer degradation by DBU base

Table 3
Thermal parameters of copolymers and grafted copolymers determined by DSC thermograms.

Copolymers/Grafted copolymers[a]	T_g (°C)	T_m (°C)
P(εCL)	Nd[b]	50.9
P(αClεCL-*ran*-εCL)		
P(**10**αClεCL-**90**εCL)	−74.7	35.2
P(**20**αClεCL-**80**εCL)	−52.6	36.4
P(**30**αClεCL-**70**εCL)	−55.9	12.1
P(αN$_3$εCL-*ran*-εCL)		
P(**10**αN$_3$εCL-**90**εCL)	−58.1	37.8
P(**20**αN$_3$εCL-**80**εCL)	−46.8	17.6
P(**30**αN$_3$εCL-**70**εCL)	−49.9	19.7
P((Nico-*g*-εCL)-*ran*-εCL)		
P((**10**Nico-*g*-εCL)-**90**εCL)	−30.1	38.6
P((**20**Nico-*g*-εCL)-**80**εCL)	−27.5	–[c]
P((**30**Nico-*g*-εCL)-**70**εCL)	−13.6	–
P((PABA-*g*-εCL)-*ran*-εCL)		
P((**10**PABA-*g*-εCL)-**90**εCL)	−41.0	37.1
P((**20**PABA-*g*-εCL)-**80**εCL)	−13.2	–
P((**30**PABA-*g*-εCL)-**70**εCL)	−5.6	–
P((Phatryp-*g*-εCL)-*ran*-εCL)		
P((**10**Phatryp-*g*-εCL)-**90**εCL)	−15.1	–
P((**20**Phatryp-*g*-εCL)-**80**εCL)	–	–
P((**30**Phatryp-*g*-εCL)-**70**εCL)	–	–

T_g and T_m stand for glass transition and melting temperatures, respectively.
[a] Abbreviations: Nico = nicotinic acid, PABA = *p*-aminobenzoic acid, Phatryp = phthaloyltryptophan.
[b] Nd = Not determined.
[c] – = no peak observed.

catalyzed nucleophilic ester cleavage in the polymer backbone caused by the deprotonated amino group of the PABA aniline fragment. This is leading to intra- and intermolecular transesterifications.

When the milder base triethylamine (TEA) was used instead of DBU, the extent of degradation of the easily degraded polymer backbone was diminished. Therefore, TEA was further on used in this study, leading to successful grafting PABA onto the polymer chain. Under this modified condition the grafted copolymers at 20 and 30% showed molecular weights which increased with the same molecular weight distribution as compared to P(αN$_3$εCL-*ran*-εCL) (Table 2). The GPC chromatogram confirmed this result with a unimodal in stead of the bimodal peak.

The grafted copolymer was characterized by the ^{1}H NMR signal of the methyne proton of the triazole ring at 7.65 ppm and those of the benzene protons of PABA at 6.65 and 7.85 ppm (Fig. 5B). The

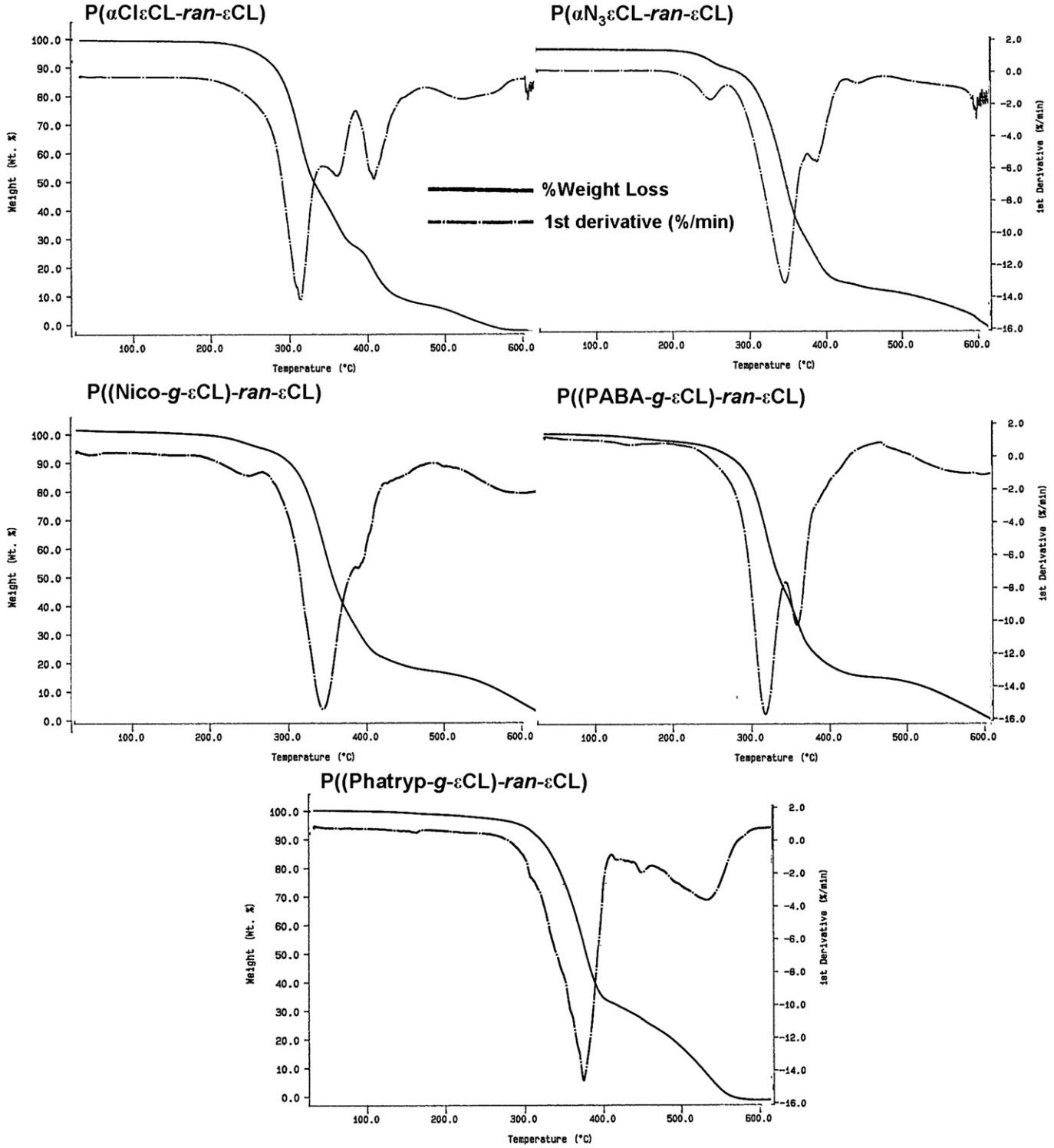

Fig. 7. TGA profiles of copolymers and grafted copolymers at 20% molar ratio (— = %weight loss; —·—· = 1st derivative).

grafting was also confirmed by the FTIR spectrum with bands for N–H stretching at 3400 cm^{-1}, C=N stretching of the triazole ring at 1626 cm^{-1}, and C=O stretching of the polyester polymer and ester bond of the pendent PABA, at 1700 and 1725 cm^{-1}, respectively (Fig. 4B).

3.5.3. *Grafting of phthaloyltryptophan by means of 3(2-N-phthalimido-2-(prop-2-ynyl acetayl)ethyl)indole (3) along the P(εCL) backbone*

The phthaloyltryptophan by means of *3(2-N-phthalimido-2-(prop-2-ynyl acetayl)ethyl)indole (3)* was used as a large and bulky representative to investigate the limitation of grafting onto P(εCL) backbone through click reaction. However, this compound could be completely attached along P(εCL) after 4 h using the same conditions as for engrafting of nicotinic acid. The ^1H NMR spectrum showed the characteristic signal of triazole proton (Fig. 5C), together with the typical set of signal groups of phthaloyltryptophan between 6.9 and 8.0 ppm coinciding with the absence of methyne proton signal of the former azide (C*H*–N_3) at 3.85 ppm. The FTIR spectrum (Fig. 4C) also confirmed the successful click reaction by means of the N–H stretching peak at 3400 cm^{-1} and the two C=O stretching bands at 1710 and 1774 cm^{-1} of the phthaloyl group.

The molecular weight of the grafted copolymer calculated from ^1H NMR and GPC gradually increased according to the increasing number of grafted units. Its distribution was narrower than that of P(αN_3εCL-*ran*-εCL) (Table 2). Unlike to the grafted PABA, DBU did not cause any severe chain degradation according to GPC results, since the indole ring proton is less acidic and sterically hindered by the phenyl ring and hardly converted to the nucleophilic species. However, this steric effect did not disturb the completeness of grafting reaction. In contrast, Riva et al. [12] were only able to engraft a linear macromolecule, PEO, on the P(εCL) backbone to just 40% probably due to stronger sterical interaction between two macromolecules than in the case of phthaloyltryptophan with complete of engrafting.

3.6. *Thermal properties of the copolymers and grafted copolymers*

The thermal properties of the grafted copolymers were measured with DSC and TGA and compared to those of the original P(αN_3εCL-*ran*-εCL) and P(αClεCL-*ran*-εCL). The glass transition temperature T_g and melting temperature T_m values characterizing the polymorphic properties of the copolymers are summarized in Table 3 indicating their semisolid form. In case of an undetectable T_ms the polymer is amorphous. In some cases of destructible polymers T_gs cannot be detected. The T_gs values of P(αN_3εCL-*ran*-εCL) and of P(αClεCL-*ran*-εCL) tend to increase with increasing molar ratio of substituted units, meanwhile their T_ms tend to decline.

The increase of grafted units in the copolymer resulted in the change of the polymorphic form from semi-crystalline to amorphous, altering their thermal properties. At 10% grafting of nicotinic acid and PABA, respectively, the T_m was observable while at higher ratios it was undetectable. In case of grafting phthaloyltryptophan, T_m was not detected at all grafting ratios. Thus, conversion from polymorphic to amorphous form of these kinds of copolymers goes with their size and/or with the increasing number of substituted units.

To investigate the thermal degradation of the copolymers in comparison with the grafted copolymers, TGA profiles were recorded. Fig. 7 illustrates TGA profiles of copolymers and grafted copolymers at 20% molar ratio. The thermograms of P(αN_3εCL-*ran*-εCL) and P(αClεCL-*ran*-εCL) show different thermal degradation pattern. Although, the starting degrading temperature of both copolymers at around 200 °C was similar, in case of P(αClεCL-*ran*-εCL) the main degradation peak appeared at around 335 °C followed by a small degradation peak, a moderate degradation peak at 370 °C, and by a small broad degradation peak starting at 460 °C. In contrast, P(αN_3εCL-*ran*-εCL) showed a small degradation peak at 270 °C attributed to the initial rupture of azide (N–N_2) [36,37] and an extensive weight loss was found at 350 °C followed by moderate degradation peaks at 400 °C. In case of the grafted copolymers, the thermal degradation pattern of P((Nico-*g*-εCL)-*ran*-εCL was the same as that of P(αN_3εCL-*ran*-εCL). The thermogram of P((PABA-*g*-εCL)-*ran*-εCL exhibited only two main degradation peaks, an extensive at 320 °C and a moderate one at 370 °C. the latter one being stronger than that of P(αN_3εCL-*ran*-εCL) at comparable temperature. For P((Phatryp-*g*-εCL)-*ran*-εCL, the extensive degradation started at 370 °C while the second degradation step was shifted to about 550 °C. According to these results all copolymers and grafted copolymers are thermally stable to about 200 °C in dried state.

From these combined results it can be concluded that the thermal properties of the grafted copolymers are largely governed by the type of grafted bioactive model compound at the polymer backbone. The larger bioactive molecule altered the thermal properties stronger than the smaller type. In addition, an increasing amount of grafted model compound changed the structure of the grafted copolymer to the amorphous form.

4. Conclusion

Three bioactive model compounds (nicotinic acid, PABA, and phthaloyltryptophan) were successively grafted onto the P(εCL) backbone through copper-catalyzed Huisgen's 1,3-dipolar cycloaddition or the "click reaction". Under very mild conditions, the reaction could preserve the length of the polymer backbone. However, reflecting the type of the model compound containing either a protic or a nucleophilic group the type of base used in the reaction is the critical issue since in combination they may possibly lead to intra- or intermolecular transesterification and thus induce the polymer chain degradation. Several types of model compounds could be grafted along the polymer backbone by varying amounts of the αClεCL units on the backbone. The molecular size of the compounds modified the physicochemical and thermal properties of the grafted copolymers compared to the copolymer. The grafted copolymers could be identified by FTIR, NMR, and GPC analysis. Derived from this accomplishment, various kinds of drugs including cytotoxic drugs, peptides and proteins, could probably be grafted along the polymer backbone in ongoing research in order to modify the physicochemical properties of drugs and also of macromolecular carriers to be more suitable for drug delivery applications. The conjugation of these grafted copolymers with other polymeric carriers such as PEG and nanoparticles prepared from these grafted copolymers are being under investigation to gain more efficient drug delivery systems.

Acknowledgements

Financial support from the Thailand Research Fund (TRF) through the Royal Golden Jubilee Ph.D. Program (Grant No. PHD/0189/2547) and the Thai Research Fund and Commission of Higher Education, Thailand for the research funding (RMU5180019) is gratefully acknowledged. The authors are very pleased to acknowledge the National Metal and Materials Technology Center (MTEC, Pathumthani, Thailand) for GPC experiment. The authors thank Professor Dr. AW Frahm, Department of Pharmaceutical and Medicinal Chemistry, Institute of Pharmaceutical Sciences, Freiburg University, Freiburg, Germany, for language and writing approval.

Appendix. Supplementary material

Supplementary data associated with this article can be found, in the online version, at doi:10.1016/j.polymer.2010.03.034.

References

[1] Lee JS, Go DH, Bae JW, Lee SJ, Park KD. J Control Release 2007;117(2):204–9.
[2] Park EK, Kim SY, Lee SB, Lee YM. J Control Release 2005;109(1–3):158–68.
[3] Jubo L, Payam Z, Faquan Z, Christine A. J Pharm Sci 2008;97(8):3274–90.
[4] Shi Q, Chen X, Lu T, Jing X. Biomaterials 2008;29(8):1118–26.
[5] Kulbokaite R, Ciuta G, Netopilik M, Makuska R. Reactive Funct Polym 2009;69 (10):771–8.
[6] Börner HG. Prog Polym Sci 2009;34(9):811–51.
[7] Trollsas M, Lee VY, Mecerreyes D, Lowenhielm P, Moller M, Miller RD, et al. Macromolecules 2000;33(13):4619–27.
[8] Rieger J, Bustele KV, Lecomte P, Detrembleur C, Jérôme R, Jérôme C. Chem Commun (Camb) 2005;2:274–6.
[9] Lecomte P, Riva R, Schmeits S, Rieger J, Butsele KV, Jérôme C, et al. Macromol Symp 2006;240:157–65.
[10] Pitt CG, Gu Z-W, Ingram P, Hendren RW. J Polym Sci A Polym Chem 1987;25 (4):955–66.
[11] Lutz J-F, Zarafshani Z. Adv Drug Deliv Rev 2008;60(9):958–70.
[12] Riva R, Schmeits S, Jérôme C, Jérôme R, Lecomte P. Macromolecules 2007;40 (4):796–803.
[13] Riva R, Lussis P, Lenoir S, Jérôme C, Jérôme R, Lecomte P. Polymer 2008;49 (8):2023–8.
[14] Zednik J, Riva R, Lussis P, Jérôme C, Jérôme R, Lecomte P. Polymer 2008;49 (3):697–702.
[15] Lee R-S, Huang Y- T. J Polym Sci A Polym Chem 2008;46(13):4320–31.
[16] Chen A-L, Ni H-C, Wang L-F, Chen J- S. Biomacromolecules 2008;9 (9):2447–57.
[17] Pertuit D, Moulari B, Betz T, Nadaradjane A, Neumann D, Ismaïli L, et al. J Control Release 2007;123(3):211–8.
[18] Bingham S, Cummings JH. Clin Sci (Lond) 1983;64(6):629–35.
[19] Brueckner B, Boy RG, Siedlecki P, Musch T, Kliem HC, Zielenkiewicz P, et al. Cancer Res 2005;65(14):6305–11.
[20] Guo B, Zhou X, Xiao X, Li J, Li L. Hua Xi Kou Qiang Yi Xue Za Zhi 2001;19 (5):315–7.
[21] Iinuma I, Uyama S, Uenoyama K, Sakaguchi T. Nippon Ganka Gakkai Zasshi 1961;65:1463–7.
[22] Jakobsen J, Pedersen AN, Ovesen L. Eur J Clin Nutr 2003;57(1):138–42.
[23] Pahan K. Cell Mol Life Sci 2006;63(10):1165–78.
[24] Safeer RS, Lacivita CL. Am Fam Physician 2000;61(11):3371–82.
[25] Siedlecki P, Boy RG, Musch T, Brueckner B, Suhai S, Lyko F, et al. J Med Chem 2006;49(2):678–83.
[26] p-Aminobenzoic acid. In: Windholz M, Budavari S, editors. The Merck index. 10th ed. New Jersey: Merck & Co., Inc.; 1983. p. 62–3.
[27] Kern CJ, Antoshkiw T, Maiese MR. Anal Chem 2002;20(10):919–22.
[28] Nefkens GHL. Nature 1960;185(4709):309.
[29] Nefkens GHL, Tesser GI, Nivard RJF. Recl Trav Chim Pays Bas 1960;79: 688–98.
[30] Lenoir S, Riva R, Lou X, Detrembleur C, Jérôme R, Lecomte P. Macromolecules 2004;37(11):4055–61.
[31] Mizrahi DM, Waner T, Segall Y. Phosphorus, Sulfur Silicon Relat Elem 2001;173(1):1–25.
[32] Zeng Q, Liu Z, Li B, Wang F. Amino Acids 2004;27(2):183–6.
[33] Gil MV, Are'valo MJ, Lopez O. Synthesis 2007;2007(11):1589–620.
[34] Im YJ, Gong iH, Kim HJ, Kim JN. Bull Korean Chem Soc 2001;22(9):1053–5.
[35] Oediger H, Möller F, Eiter K. Synthesis 1972;1972(11):591–7.
[36] Ero MS, Güven O. J Appl Polym Sci 1996;61(2):201–6.
[37] Fazlloglu H, Hacaloglu J. J Anal Appl Pyrol 2002;63(2):327–38.